Marker-referred movement measurement with grey-scale coordinate extraction for high-resolution real-time 3D at 100 Hz

E. Hans Furnée [a], Akos Jobbágy [b], Jan Cees Sabel [ac], Hans L.J. van Veenendaal [ad], Ferenc Martin [b], Denie C.W.G. Andriessen [a]

[a] Delft Univ. of Technology, Motion Studies Lab., PO Box 5046, 2600 GA Delft, Netherlands
[b] Technical Univ. of Budapest, Meas. & Instr. Eng., Muegyetem rkp. 9, 1521 Budapest, Hungary
research work partly carried out as a research fellow at Delft University of Technology
[c] presently at TNO Physics & Electronics Lab., the Hague, Netherlands
[d] presently at SEGA Enterprises, Tokyo, Japan

ABSTRACT

A review of early history in photography highlights the origin of cinefilm as a scientific tool for image-based measurement of human and animal motion. The paper is concerned with scanned-area video sensors (CCD) and a computer interface for the real-time, high-resolution extraction of image coordinates of moving markers. Algorithms and implementations are reviewed for the estimation of marker midpoints. Two-valued (above-threshold) representations of the video signal, as well as grey-scale digitizing are discussed. Attainable resolutions and computational effort are presented. Distributed, per-camera processing is a new option, which uses an embedded microcomputer for image reduction to real-time marker midpoint data. Developments are discussed in 3-D camera calibration and in the real-time 3-D matching of marker images, essential in real-time 3-D reconstruction. Applications are in 3-D motion capture for animation and in motion analysis of wind turbine rotors.

Keywords: markers, embedded image processing, coordinates, location, grey-scale processing, sub-pixel resolution, marker tracking, 3D, real-time, motion capture, animation, wind turbines, motion analysis.

1. INTRODUCTION

1.1 Photography and cine-film in early movement measurement.

Image-based motion measurement dates back more than a century when the early art of photography was introduced to human and animal locomotion studies.
It was the British photographer Eadward Muggeridge (later Muybridge) who in Sacramento, California, USA demonstrated the ability of photography to arrest motion by a sequence of pictures. With an array of 12 cameras, with trip-wired shutters to secure properly ordered delay, he in 1872 proved the unsupported transit phase of the horse in trot: a wager had been laid on the number of hooves in contact with the turf. Muybridge later incorporated electromagnetic shutters and sequential triggering of up to 24 cameras by a rotary commutator. His heritage of serial photography consists of some 100.000 plates of animal and human motion recorded at Palo Alto, California and, from 1884, at the University of Pennsylvania [1].
As an early effort in numerical motion analysis, by 1888 Dercum [2] had already presented displacement-time curves for normal and pathological gait which were derived from Muybridge's recordings.

Some improvements to Muybridge's multi-camera single-exposure system were due to the French engineer-physiologist Etienne-Jules Marey [3], such as his version of the photographic gun. Here, once it is triggered, a chamber loaded with 12 pieces of photographic emulsion rotates at high speed behind a barrel-like lens holder. The chamber came to intermediate full stops for exposure. This made serial exposures within 1 s, with aperture times of 1/720 s. Using three such cameras Marey obtained three perpendicular projections of ten phases of a seagull in free flight.

Author information: [a] E.H.F.: email: furnee@tn.tudelft.nl; Telephone: 0031-15-278.5996; FAX: 0031-15-278.4263
[b] A.J.: email: jobbagy@mmt.bme.hu; Telephone: 0036-1-463.2275; FAX: 0036-1-463.4112

Marey (op.cit.) was aware of stroboscopy, as already used by Savart in the optical subsampling of periodic phenomena by exploiting the eye's image retention. Marey extended the method to photography with what he called photochronography, where he incorporated a rotary disk shutter with one or more slits inside the single plate camera. In discussing stroboscopy, he was well aware of the possibilities offered by periodic illumination by what was then the technology of spark discharges. With his shuttered photochronography instrument Marey recorded human movement with subjects dressed in white contrasted against dark backgrounds, thus obtaining a time decomposition of, for example, pole-vaulting as in his 1894 book [4].
To obtain pictures less crowded with unmanageable detail, Marey went on to dress his subjects in black, with limbs and head marked by stripes and buttons shining in the sun. Thus his subject was reduced to an abstract representation of complex progressive motion. This is how photochronography produced the first of what were later called stick diagrams (fig. 1).

Observing that the pictures, taken at successive time instants, tended to crowd on top of each other if the subject did not move enough, Marey installed a moving mirror inside the camera to spread the images out across the sensitive surface. He then thought of moving the plate itself. In his chronophotographic box, presented 1888 to the Paris Academy of Sciences, Marey indeed had a strip of photographic paper transported at 20 exposures/s behind the lens and rotary shutter mechanism. Again, Marey was aware of the necessity of the film being at rest during each of the successive exposures, and he described the transport mechanism employed. In his 1890 book, Marey [5] mentions a sensitive celluloid film, employed at a rate of 50 exposures/s with aperture times of 1/4000 s: the film camera was born, and it was originally a scientific research instrument. These Marey cameras were developed and reported years earlier than W.K.L. Dickson's kinetoscope at the Edison factory in the USA. The Dickson camera in turn pre-dated by three years the much more publicised cinematograph of the French Lumière brothers: this signalled the birth of cinema as an entertainment and educational medium.

For the better part of the 20th century, cine-film remained the method of choice in human and animal movement studies and, evolved into high-speed photography, the technology retains a valid place, as witnessed by contemporary SPIE Conferences.

Also, Marey's approach to represent and generalize his moving subjects by a collection of contrasting dots and stripes: physical markers fixed to anatomical landmarks, has remained a cornerstone method in image-based movement analysis.

Specific, often high-speed, areas exist where the imaging and analysis concerns isolated, albeit often very many, objects. Examples are in ordnance or in fluid dynamics, with no significance attached (or instrumental access) to the dimensionality of these objects, or to other than their translational degrees of freedom.
However, a vast research and applications area of image-based motion measurement addresses the medical, industrial and even entertainment interest in the movement and/or deformation of objects which have appreciable dimensions, and where objects are in many cases articulated, and may then be represented by solid-body linked-segments. It is specifically in this application area that the objects are characterized by markers. Here, the markers as imaged are basic to motion measurement.

1.2 Computing and sensor-based motion measurement systems

The mid-1960's have seen the first attempts to transcribe or encode cine-film into computer data. For frame-by-frame digitization, the moving images as recorded were to a large extent marker-based, for convenience in manual operation, or by necessity in semi-automated modes. This technology concerns the time-dependent marker coordinates for motion analysis.

Similarly aimed at the extraction of the coordinates of moving markers, but skipping the cine-film process, the first real-time, camera-based video-to-digital coordinate converter was demonstrated by Furnée (1967) from Delft University of Technology. [6] Basically in this system, the video signal is compared to a selectable threshold, and at each threshold crossing the coordinates of the corresponding image point are established by copying to memory the instant count value of two running counters. These counters are rigourously synchronized to the camera, or alternatively these counters supply the camera sync. The line counter supplies the vertical or Y coordinate, the horizontal or X counter is run on the pixel clock. Immediately after the threshold comparator, which can be considered a 1-bit A/D conversion, the system is fully digital, and feeds into a computer.

The ensuing three decades have seen the continued development as from the TU-Delft prototype, as well as, since the early 1980's the emergence both of academic look-alikes and of commercially competitive motion analysis systems, mainly applied within biomechanics. The evolutionary state-of-the-art was (1990) represented at the first SPIE-Symposium on Image-Based Motion Measurement [7]. Vicon (1981), ELITE (1985), ExpertVision are main brand names along with Delft PRIMAS systems.

Another early TV camera-based system [8] was of a slightly different category in image-based motion measurement. CINTEL was basically a 5-bit digitiser of video amplitude on a selected, and by reason of conversion speed reduced, grid of image points. As such it can be considered the primordial framegrabber, at a time too early for industry to realize its potential. Basically, in a framegrabber system each grid point or the corresponding memory address represents an image coordinate pair, on a pixel boundary in current CCD terminology. And for the ensuing problem-oriented pattern processing, such as for marker geometry and location, the software to read the relevant pixel video values must access all memory addresses. This is not so in the video-to-digital coordinate converters, essentially no framegrabbers, which are the subject of this paper.

2. PRIMAS Precision Motion Analysis System

2.1 Main system components

To focus on a representative system, with an innovation track record in marker image based motion measurement, the following is a breakdown into main components of the PRIMAS Precision Motion Analysis System:

1. Markers, strategically attached to the subject.
2. one or more Cameras, each with an IRED illuminator, which is centered around the camera lens.
3. PRIMAS Marker Processor, comprising: a. multi-camera video-digital coordinate converter.
   b. multi-camera marker centre estimator.
4. Host PC, interfaced to the PRIMAS Marker Processor.

The ***markers*** as mentioned in the introduction are the prime concern in any motion analysis system and, within the CCD camera-based system category, the markers are low-inertia non-wired, passive retro-reflectors. The markers within the field of view (FOV) are irradiated with infrared, by rings of IR-LED's centered around the camera lens. The irradiation is stroboscopic by short flash pulses synchronized to the camera field rate.
The ***cameras*** are dedicated in that they are electronically shuttered so as to feature a 0.25 ms integration time. Combined with the IR strobing, this results in a 1:40 suppression of ambient or background light and a high contrast of the marker images even in outdoors full daylight. These cameras run at 100 Hz (100 fields/s, non-interlaced).
The ***PRIMAS Marker Processor*** is implemented to serve 6 cameras. Optionally, 2 other cameras can be selected. Per camera, the analog video signal is fed to a comparator with an adjustable threshold reference, to produce binary or above-threshold video which expresses and is limited to the marker images or 'blobs'. Each of the 6 ***video-digital coordinate converters***, as introduced in section 1.2, consists of digital counters, one for line number Y and one for pixel number X. These counters are fully synchronous to the main system controller that synchronizes the cameras down to the pixelclock level. The instant read-out of the running X,Y counters at the binary video transitions produces the digital X,Y coordinate values at the imaged marker contour points on the pixel grid.
Per camera, the marker contour coordinates so obtained are buffered, per image field, and subsequently processed in the central ***marker centre estimator*** subsystem. The current implementation is on a 68030 VME-based embedded CPU, while much similar results were obtained with a 16 MHz R-3000 RISC subsystem. Interrupt-driven by the 100 Hz field sync, this real-time processor runs at a 100 Hz heartbeat, with a throughput of some 200 midsized markers or 33 as seen by 6 cameras.

The objectives of marker centre estimation are:
a. further real-time data reduction and
b. sub-pixel definition (resolution, accuracy) of the centre coordinates of the markers.

For the purpose of sub-pixel resolution the markers are large enough to be imaged across several lines on the CCD pixel grid [9] [10]. Real-time marker processing is among the early features in the PRIMAS system development [11] [12] [13].

From the marker centre estimator, the coordinate output data are interfaced to the host PC. The 10MByte/s serial ***interface*** is based on the AMD-TAXIchipset (Transparent Asynchronous Xmitter-Receiver Interface), with a proprietary ISA-board. In duplex, this interface also links the PC to the Marker Processor for menu-driven control of camera and threshold options. The ***host PC*** is a -486 or Pentium, ISA-bus compatible, running the PRIMAS data acquisition and control programs READ or NEWREAD under MS DOS, alternatively WINREAD under MS Windows-95.

NEWREAD and WINREAD both have a proprietary real-time 3-D matching kernel by HLJvV. With its Ethernet and serial sockets this allows PRIMAS system use as the first image-based real-time 3-D motion capture channel in live computer animation [14] and -outside the entertainment industry- as the real-time 3-D sensor in motion control technology.

The paper's emphasis is on the marker centre estimator, on distributed, per-camera marker processing and on real-time 3-D.

2.2 Marker centre estimation

One basic method for centre estimation of a marker image, as represented by above-threshold video on a pixel grid (fig. 2), is the estimation of the geometric centroid [10]. With the coordinates of a segment, denoting an elementary row of above-threshold pixels, as in fig. 2, the basic equations are

$$X_{0g} = \frac{\sum_{i=1}^{L} (X_{2i} - \frac{dX_i}{2}) dX_i}{\sum_{i=1}^{L} dX_i} \quad , \quad Y_{0g} = \frac{\sum_{i=1}^{L} Y_i dX_i}{\sum_{i=1}^{L} dX_i} \qquad (1)$$

where L is the number of segments, and

$$\textit{Where } dX_i = X_{2i} - X_{1i} \quad \textit{(segment length) and } X_{2i} - \frac{dX_i}{2} = \frac{X_{1i} + X_{2i}}{2} \quad \textit{(mid-segment)}$$

The video-digital coordinate-converter hardware like reviewed in 2.1 outputs the X_{2i}, dX_i and Y_i values. The marker centre estimator output are the (X_{0g}, Y_{0g}) values in real-time [11], the index g denotes the geometric centroid approximation.

Illustrative already of sub-pixel resolution, fig. 3 the result of encompassing simulations shows, as the curve S1 (1-bit binary video) the RMS error (expressed as a fraction of pixel size) vs. marker image radius (fractional multiples of pixel size).

Alternative methods have, as more or less advanced implementations of circle fitting [26], been proposed and investigated in a linear least squares approach, which was modified to allow solutions in real-time [15].

As a further alternative to basic circle fitting, a new method producing a Best Estimate Without Radius Information (BEWRI) was proposed and investigated [15] [16]. Unlike the geometric centroid estimation, the BEWRI method was shown to closely approximate the theoretical limit of accuracy (local, on the pixel grid).
As a final proposal for centre estimation of binary-valued marker images (above-threshold video representation) a new ring fitting method was investigated [16] as a simplified algorithm allowing real-time processing and approximating the accuracy of BEWRI. Moreover, the ring fitting method can process distorted marker images and inherently provides a measure for the distorsion from the ideal circular marker image. It was tentatively implemented in the RISC-based PRIMAS version (2.1).

The BEWRI method and its realisation in ring fitting have the advantage that they compensate a part of the quantization error inherent in the binary marker image on the pixel grid. Common to both methods is that the midpoint estimate is derived by considering the whole set of marker images (midpoint and radius) that can correspond to the binary image as presented.

2.3 Marker centre estimation using grey-scale video

Departing from the binary-image representation of markers, as mentioned above by above-threshold video on the pixel grid, the video intensity, or grey-scale values on the pixel grid have first been used in the primordial frame-grabber [8]. Later, as first used in a video-coordinate converter [17], digitizing the video signal was for the primary purpose of template matching by video cross-correlation. Template matching was aimed at discriminating the marker signals from spurious or background video. The estimation of the coordinates of the cross-correlation peak was also used as a marker midpoint estimate.

For the PRIMAS system, a new interest in using grey-scale video, as digitized by 8-bit A/D conversion, is not primarily to attain superresolutions but to use smaller markers than with the still straightforward, real-time method of geometric centroids.

Amplitude-weighed centre estimation can consider either all circumferential and interior points on the pixel grid, or only the boundary points. When all boundary and interior points are taken into account, for amplitude-weighting on the boundary pixels the most accurate option is that of correcting the individual boundary pixel midpoints on the basis of video amplitudes on nearest neighbours.

Simulations were run to estimate the computational burden, and not surprisingly the heaviest load (by a factor of 5 to 8) is in boundary-correcting intensity-weighing with interior points. The other methods have a processing load of 3 to 5 that of 1-bit geometric centroid estimation.

Of these other methods, the boundary method which skips (most of) the interior points uses amplitude-weighted interpolation between a boundary pixel and its nearest neighbour pixel. This aims at estimating virtual, interpolated segment boundaries which are the contour points at a predetermined level of video amplitude.
With reference to fig. 2, equation (1), which recall the 1-bit binary method, fig. 4 represents a cross-section of a marker segment, where the video amplitudes are interpolated between the values a and b, viz. c and d at 2 pixels on both boundaries. Here, the X_1 and X_2 values are no longer pixel boundaries, but intermediate sub-pixel coordinate values, and as such these can be used similarly to equation (1) to now obtain an interpolated-boundary center estimate.
As an alternative to the estimation of the Y midpoint in equation 1, a similar approximation to that for the X-midpoint could be used. Alternatively to figs. 2 and 4, this then implies vertical segments across the pixel grid.

Fig. 3 represents the simulated error results with the interpolated-boundary method. As noted in 2.2 with 1-bit binary video there is no amplitude difference for the above-threshold pixels, so the S1 curve represents the geometric centre estimator. The improvement with the interpolated-boundary method is already noticeable with a 2-bit video digitizing. The advantage becomes impressive with 4-bit, while 8-bit appears already in the overkill category even for the smallest markers considered.

3. IMAGE-PROCESSING CAMERA

The new generation of PRIMAS cameras with embedded image processor features the simultaneous storage of selected A/D converted video and the corresponding pixel coordinates. As such they are no framegrabbers in the sense discussed in 1.2, nor are they video encoders following current compression principles (MPEG).

The 8-bit video data selected for primary storage is restricted to video above a preset, relatively low threshold. Video selection is by digital logic acting on the ADC output. The pixel coordinates are generated by readout of line- and pixelsynchronous counters as reviewed in sections 1.2 and 2.1.
Additional on-board programmable logic and a byte-wide FIFO with the depth of one video line are the building blocks of a configurable data selector. Selectable functions are a) the additional storage of the nearest adjacent pixels for the relevant below-threshold video or b), the opposite in data reduction, the limitation to boundary pixels.
Ensuing on-the-fly processing by the embedded computer, as the final step in real-time data reduction, delivers the marker midpoint estimates according to methods discussed in section 2.3. Alternative methods like ring fitting on 1-bit binary video (section 2.2) can likewise be implemented for realistic investigations on processing load.
Essentially, the cameras as described are dedicated to produce the marker midpoint coordinates, and as such provide a minimum data output rate. An exemplary 30 markers at 4 bytes per marker at 100 Hz feed out at just 12 kByte/s. Essentially then, the multi-camera 3-D hookup is satisfied by low-cost, low-bandwidth transfer media.
As such, the cameras are high-resolution marker image (blob) locators, they bypass the Central Marker Processor as in section 2.1, and for real-time 3-D they hook up simply into the host PC or into sophisticated graphics/animation engines.

The embedded, credit card format RISC computer not readily forthcoming as announced, the present choice is a 53x82 mm low-cost 80386EX Microcontroller Module. This comes readily featured with all current peripheral controls, SRAM, Boot Flash, Flash Disk, JTAG download and with CAN (Controller Area) networking for the multi-camera interconnect.
The straigtforward, low-bandwidth hook-up favours the use of long camera baselines as in wind turbine measurement (6).

4. 3-D CALIBRATION

4.1 Calibration with Planar Control Object

3-D Calibration of a multiple-camera configuration is usually achieved by recording the images of a set of control points (i.e. points in 3-D measurement space with an accurately known position) followed by a parameter estimation procedure employing an adequate image model, that should also incorporate a lens distorsion model. Basically, 3-D calibration sets out to establish, for each of the cameras, the external and the internal camera parameters. The external parameters are relevant to the six degrees of freedom (pose) of the camera-bound coordinate system, e.g. the location of perspective point, orientation of optical axis and transverse axes in the image plane, within the coordinate system of the measurement space. The internal camera parameters are relevant to the principal point in the image plane, scale factors and parameters of lens distorsion.
The classical method employing the Direct Linear Transformation algorithm [18] with its subsequent refinements [19] requires a 3-D control object of dimensions comparable to the measurement space or field of view (FOV). This is an important practical limitation in many applications, within and outside of human biomechanics.

The calibration method adopted for the PRIMAS system is an implementation [20] of the SMAC (Simultaneous Multiframe Analytical Calibration) algorithm [21]. This employs a planar calibration object, with in the PRIMAS case 48 markers in a rectangular grid on a stiff but lightweight substrate. The calibration plane is recorded in at least three arbitrary but different poses within the common cameras' FOV. One of these poses is considered to be the reference pose defining the FOV coordinate system. Moreover, each individual camera must record one full-view observation of the calibration plane as a prerequisite for the estimation of that camera's internal parameters.
The retro-reflective markers are planar disk shaped for accurate positioning on (one side of) the calibration plane, but consequentially the control points are visible only by cameras unilateral to the calibration plane. Where this is a disadvantage, such as in bilateral observation systems which would allow full-turn rotations of the subject, recourse must be taken to multiple calibration recordings where the control plane is viewed by distinct subsets of the camera configuration. These subsets of calibration parameters must subsequently be linked by a recording where an, in this case limited number of control points are observed by all cameras. One approach to this effect is to use a small but accurately known spatial distribution of spherical markers, and alternatively to the one selected pose of the calibration plane, this auxiliary 3-D control set, such as aligned to e.g. a forceplate in the floor, could also be used for a final definition of the measurement space coordinates.

4.2 Single-Marker Calibration

The alternative for other than unilateral camera configurations is to present one single marker [22], for the purpose spherical and adequately large, at several different positions in the FOV of all cameras simultaneously. The single-ball calibration then serves to estimate the external parameters of all cameras from one simultaneous recording.
This method assumes the internal parameters of all cameras established by previous calibration like by the SMAC routine as above, and the assumption implies that all camera settings (focus, iris) are - to the relevant extent - unchanged. Moreover, a proper initial estimate is required of the external parameters of at least two cameras, such as by rough observation or also - even if roughly - retained from a previous calibration.
The single-ball method is particularly useful to recalibrate a multi-camera system in a bilateral, elliptical or circular configuration in a 360° observation space, as a fiduciary check or after repositioning (some) cameras without altering any lens settings. Best results are obtained if a large part of the measurement volume is covered by the otherwise arbitrary single-ball trajectory. The final step in single-ball calibration consists of a scaling operation, which can e.g. be derived from a simple control rod with two markers at known distances. Final figure on differential accuracy (the preservation of length between other than the original control points) is an RMS error of 1:3.000 of vertical FOV dimensions.

4.3 Stick- or Dual-Marker Calibration

Expanding on a dual-marker calibration method which has the property of inherent scaling [22], a generalization to m_s markers on a longitudinal (control) object with at least one known distance between markers was developed for a PRIMAS application with very large and distant objects, like the rotors of wind turbines [23] [24] [25].
Indicative of this 3-D "stick" calibration performance, a 3,5 mm RMS error was found on individual rotor marker positions. Relative to the 10 m rotor diameter, this agrees with the 1:3.000 FOV attained above.

5. STEREOMETRIC MATCHING OF MARKER IMAGES

5.1 Image matching

In passive-marker image-based motion measurement, the marker images and thus the marker coordinate values produced per camera and across the cameras, are inherently unidentified. This requires that the coordinate pairs obtained per image be matched to the corresponding physical marker in the multi-camera observation space, as a prerequisite to 3-D reconstruction. The process of point identification, or image matching, is basic to photogrammetry. One early solution [26] in image-based motion measurement uses inverse ray tracing, where in the 3-D observation space the physical markers are assumed on the ray intersections (or to allow some measurement error, at the midpoint of the shortest common perpendicular), as determined by a software search among the inverse rays (or observation lines) as generated. Common to this and following approaches is the ambiguity in the case that 2 cameras observe 2 markers that are (nearly) coplanar with the cameras' projection centres. In this case 4 (near) intersections are found, of which 2 correspond to actual markers and 2 to artefacts or ghosts (Fig. 5). Such ambiguities can be resolved by using more cameras, diligently positioned and poised, or by recourse to marker tracking.

5.2 Image matching using epipolar lines

As an alternative to searching in observation space among inverse rays (observation lines) from all of the cameras, the epipolar line method [27] [28] reduces the search to one in the image plane. An epipolar line is the projection onto the image plane of one camera of the observation line to a certain marker from the other camera. Searching for the corresponding marker in the first camera image can be limited to a narrow search band both sides of the epipolar line (Fig. 6). To abate the ghost problem, a third camera can be positioned such that its epipolar line on camera one image intersects the epipolar line from camera two. The search area for the matching marker in camera one is then further restricted to (the vicinity of) the intersection of the epipolar lines.

5.3 Real-time image matching by classification of epipolar lines

The above methods require more computational effort than amenable to real-time 3-D performance. The alternative method [29] is to attach to any marker imaged in any camera (index i) a classification value that corresponds to a similar value for the same marker in the other camera (index j). Basically, a pair of cameras is used, occurrence of ghost markers can be combated by using more cameras paired with the others. Any epipolar line in a camera can be extended to an epipolar plane in observation space. All possible epipolar planes have a common intersection line, the line connecting the projection centres of the cameras. The camera image of a bundle of epipolar planes will therefore be a set of (epipolar) lines which has one common point of origin $X_{j\ in\ i}$ (Fig. 7). This point is in the image plane but generally outside the image area, and it corresponds to the image of the projection centre of the other camera (note that $X_{j\ in\ i}$ will only be inside the image area if camera i 'sees' the other camera j). Summarizing, the method is an inverse one, where the epipolar line is found as a line through the marker image X_i and $X_{j\ in\ i}$ the origin point of all epipolars. The advantage of this method is that for all permutations i,j the 2-D virtual coordinates $X_{j\ in\ i}$ can be calculated in advance as a corollary to the 3-D camera calibration. Only the slope S_i of the epipolar line is calculated in real-time, for all markers imaged in all cameras. Furthermore, prior to real-time matching on the sole basis of slope values, the slope of the epipolar line in camera j must be converted to an $S_{j\ for\ i}$ value. Again the coefficients for the conversion polynomial are estimated in advance using the 3-D calibration data.

5.4 Real-time 3-D matching by classification of epipolar plane angles

The epipolar line slope method fails if cameras have parallel optical axes. Another limitation is that the range of slope values, which depends on the off-edge distance of the $X_{j\ in\ i}$ is thereby dependent on the intersection angle of the optical axes. By consequence, the classification or decision threshold must be adapted accordingly. The more elegant method to obviate these limitations is to perform the matching in 3-D space by identification of the epipolar plane occupied by any marker as imaged in cameras i, j respectively. For any marker, the observation vector v_i (or inverse ray) has to be calculated anyway for the ensuing 3-D reconstruction in real-time (which is by forward intersection rather than by DLT). Evidently, v_i is in the relevant epipolar plane, so v_i is used in a simple real-time equation to yield the classification value for the slope of the epipolar plane. Moreover, the equations are symmetric and require no conversion for cameras j to i, favourable to real-time matching [30]. The method, hitherto unpublished, is due to HLJvV and implemented in NEWREAD and WINREAD real-time 3-D kernels.

6. APPLICATIONS

Real-time 3-D output in image-based motion measurement was first demonstrated with PRIMAS [14] in a 1993 setting for live animation in computer graphics. This has initiated applications in the entertainment and commercials' industry worldwide.

High-accuracy 3-D is the challenging application with large-scale industrial objects, like rotor blade motion in wind turbines.

The project "3-D Motion Analysis in Full Scale Wind Turbines" addresses crucial technical aspects in the assessment and testing of new designs and development in the next generation of wind turbines. These are characterized by increasing size and increasingly flexible structures. The dynamics of rotor blades, as well as their interaction with the hub, tower and nacelle structures must be well understood in the design phase, and must be fully validated by experiment on the full-scale product. Structural fatigue and the risk of dramatic failure must be at an absolute minimum to warrant social and environmental acceptance, without which there is no economic future.

Current experimentation on rotor blade motion is limited to specially instrumented prototypes, the sensors being of the strain gauge and accelerometer type. These are attached onto the structures under test either at the surface or into specially machined cavities. Both by this fact plus by the necessary wiring and elaborate electric collector structures at the hub, these methods exert a generally unaccountable influence on the test object behaviour. Moreover, to apply this kind of active sensors requires the rotorblades to be dismounted: consequentially these existing methods are time-consuming and uneconomic for these and other reasons.
Image-based motion measurement removes the physical sensors and wiring from the rotor blades, and instead uses a set of passive optical markers. Markers are sub-millimeter thin retro-reflective foil stick-ons to the rotor surface. By implication, the remote camera/computer method can be applied to otherwise unprepared structural prototypes as well as to standard production samples. This rapid turnover facility shall benefit the penetration of an encompassing test and verification programme in wind turbine design and certification, and contribute to a better and dependable, economic and safe product.

Figs. 8 and 9 present pilot results [25] on flap motion in a 10 m diameter two-blade rotor. Flap angle is defined as the angle between the rotor axis direction and the direction of the blade minus 90° (the flap angle can be considered the bending angle of the rotor blade out of the 90° rotor plane). Apart from the longitudinal blade torsion, the flap angle is the most demanding of angles to be determined in 3-D. These tests were performed under minimum wind conditions, the small flap angles exhibit maximum noise. For test reasons the turbine had two different blades, this explains the angular offset as well as a difference in the spectral peak heights between blades 1 and 2. The 180° azimuthal phase shift between rotor blades is also evidenced.

ACKNOWLEDGEMENTS

Part of this work was supported by the European Commission, program INCO/Copernicus, contract CIPA.3510-CT93-7845, and by the International Cooperation Program of Delft University of Technology and the Technical University of Budapest. The wind turbine project was continued under the European Commission program CRAFT/Joule, contract JOR3-CT96-1004.

REFERENCES

1. Muybridge, E. (1887). Animal locomotion. Reprint in: Animals in motion. London, Chapman & Hall, 1899, 264 p; re-edited L.S. Brown, Dover 1957.

2. Dercum, F.X. The walk in health and disease. In: Trans.Col.Physicians **10**, p 308-338, 1888.

3. Marey, E.-J. La méthode graphique dans les sciences expérimentales et particulièrement en physiologie et en médecine. Paris, Masson 1872. 2nd Ed. with Supplement: Le dévéloppement de la méthode graphique par l'emploi de la photographie. Paris, Masson, 500 + 60 p, 1885.

4. Marey, E.-J. Le mouvement. Paris, Masson 1894.

5. Marey, E.-J. Le vol des oiseaux. Paris, Masson, 394 p, 1890.

6. Furnée, E.H. Hybrid instrumentation in prosthetics research. In: Proc. 7th Int. Conf. on Medical & Biological Eng. Stockholm, p 446, 1967.

7. J.S. Walton (ed.). Proceedings of the Mini-Symposium on Image-based Motion Measurement. 31 august-1 september 1990, La Jolla, CA, USA. SPIE **1356**, 144 p, 1990.

8. Dinn, D.F., D.A. Winter and B.G. Trenholm. CINTEL - Computer Interface for Television. IEEE Trans. on Computers, p 1091-1095, 1970.

9. Winter, D.A., R.K. Greenlaw and D.A. Hobson. TV-computer analysis of kinematic data of human gait. Comp.&Biomed.Res. **5**, p 498-504, 1972.

10. Taylor, K.D., F.M. Mottier, D.W. Simmons, W. Cohen, R. Pavlak Jr, D.P. Cornell and B. Hankins. An automated motion measurement system for clinical gait analysis. J. Biomechanics **15** # 7, p 505-516, 1982.

11. Furnée, E.H. Intelligent movement-measurement devices I: video converter with real-time narker processor. In: Proc. 8th Int. Symp. on External Control of Human Extremities, Dubrovnik / ETAN Belgrade, Supp. p 39-41, 1984.

12. Furnée, E.H. High-resolution real-time movement analysis at 100 Hz. In: Proc. North American Conf. on Biomechanics. Montreal, p 273-274, 1986.

13. Furnée, E.H. PRIMAS: real-time image-based motion measurement system. In: (J.S. Walton ed.) Proc. Mini-Symposium on Image-based Motion Measurement. SPIE **1356**, p 56-62, 1990.

14. Furnée, E.H., J.C. Sabel, H.L.J. van Veenendaal and Oshri Even-Zohar. Animotion. Human motion capture for live animation. Technical Exhibit, booth 24, 14th Congress of the Int. Soc. of Biomechanics, Paris july 4-8, 1993.

15. Jobbágy, A. and E.H. Furnée. Marker centre estimation of high accuracy in motion analysis. J.of Medical and Biological Engineering and Computing **32**, p 85-91, jan. 1994.

16. Jobbágy, A. Centre estimation in marker based motion analysis. PhD Thesis Technical University of Budapest. No. TUB-TR-EE04. ISBN 9634215092. Budapest, 90 pp, april 1993.

17. Ferrigno, G. and A. Pedotti. ELITE: a digital dedicated hardware system for movement analysis via real-time TV signal processing. IEEE Trans.on Biomedical Electronics **BME-32**, p 943-950, 1985.

18. Marzan, G.T. and H.M. Karara. A computer program for Direct Linear Transformation solution of the colinearity condition and some applications of it. In: Proc. Symp. Close-range Photogrammetric Systems. Champaign, p 420-426, 1975.

19. Hatze, H. High precision three-dimensional photogrammetric calibration and object space reconstruction using a modified DLT-approach. J. Biomechanics **21** # 7, p 533-538, 1988.

20. Sabel, J.C. Implementation of SMAC (Simultaneous Multiframe Analytical Calibration) in a 3D motion analysis system. EU-AIM-CAMARC Deliverable M, p 153-158, 1990.

21. Woltring, H.J. Simultaneous Multiframe Analytical calibration (S.M.A.C.) by recourse to oblique observations of planar control distributions. In: Proc. NATO Conf. Applications of Human Biostereometrics. SPIE **166**, p 124-135, 1978.

22. Sabel, J.C. Camera calibration with a single marker. In: Proc. 3rd Int.Symp. on 3D Analysis of Human Movement. Stockholm, p 7-9, 1994.

23. Sabel, J.C. Optical 3D Motion Measurement. In: Proc. Joint Conf. IEEE-Instrumentation and Measurement Technology Conf.& IMEKO Techn. Committee 7, Vol. 1, IEEECatalog# 96CH35936, ISBN 0780333128, p 367-370, 1996.

24. Corten, G.P. and J.C. Sabel. Optical motion analysis of wind turbines. Techn.Rept. SV Research Group, TU Delft, sept. 1995 ISBN 9075638019, 31 p, 1995.

25. Corten, G.P and J.C. Sabel. Optical motion analysis of wind turbines. The pilot experiment with the Delft 10 [m] diameter wind turbine. In: (Zervos, A., H. Ehmann and P. Helm, eds.) Proc. 1996 European Union Wind Energy Conference and Exhibition. Stephens & Ass. Felmersham UK, ISBN 0952145294, p 875-877, 1996.

26. Macleod, A., J.R.W. Morris and M. Lyster. Highly accurate video coordinate generation for automatic 3D trajectory calculation. In: (J.S. Walton, ed.) Proc. Mini-Symp. Image-Based Motion Measurement. SPIE 1356 p 12-18, 1990.

27. Baltsavias, E.P. and D. Stallmann. Trinocular vision for automatic and robust three-dimensional determination of the trajectories of moving objects. Photogrammetric Eng. & Remote Sensing 57 # 8, p 1079-1086, 1991.

28. Maas, H.G. Automated photogrammetric surface reconstruction with structured light. In: Proc.Int.Conf.on Industrial Vision Metrology, SPIE 1526, 1991.

29. Sabel, J.C., H.L.J. van Veenendaal and E.H. Furnée. PRIMAS, a real-time 3D motion analysis system. In: Proc. 2nd Conf. on Optical 3D Measurement Techniques. Zurich, p 530-537, 4-8 oct. 1993.

30. J.C. Sabel. Calibration and 3-D reconstruction with a motion measurement system. PhD thesis Delft University of Technology. Submitted to Faculty, 1997.

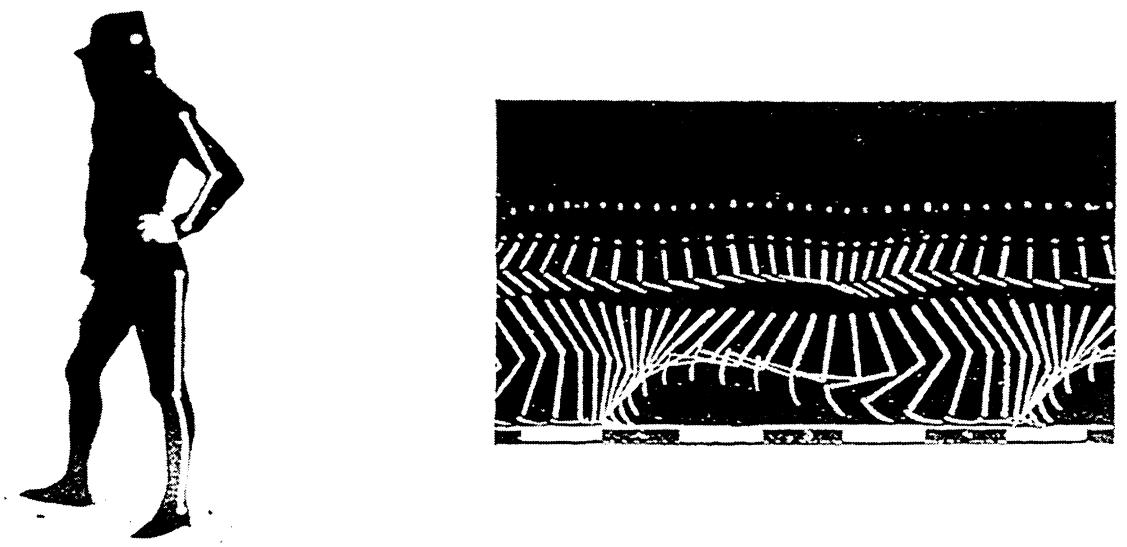

Fig. 1 Black dressed subject with markers, stick diagram (Marey).

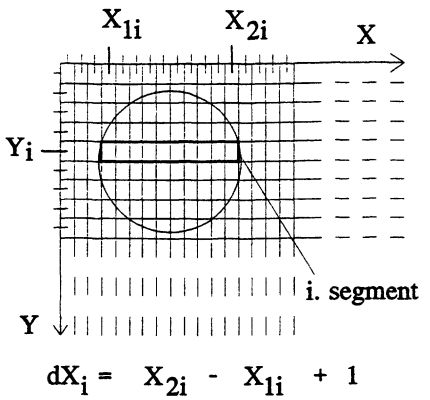

Figure 2. Marker image on pixel grid. Segment = consecutive pixels on one line

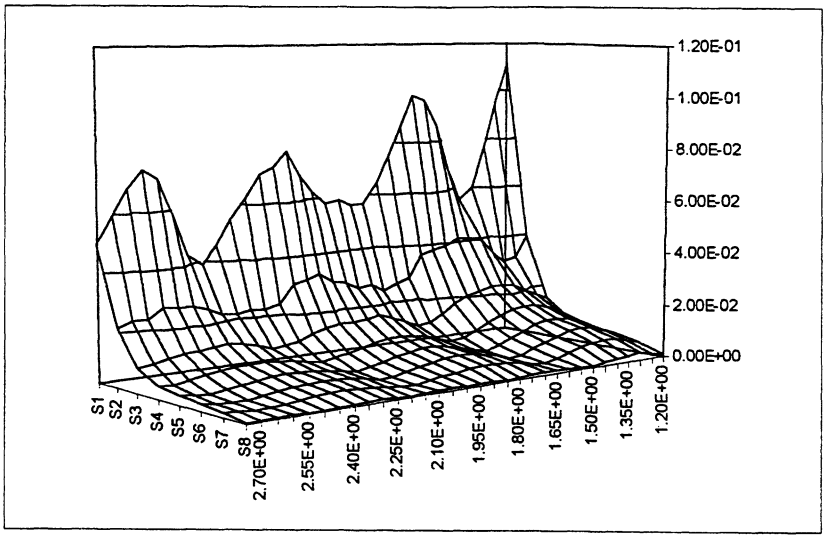

Figure 3. Error (Simulated, Vert. Axis, fraction of pixel size)
vs. Marker Radius (Hor. Axis, in pixelsize) vs. A/D converter bits (Oblique Axis)

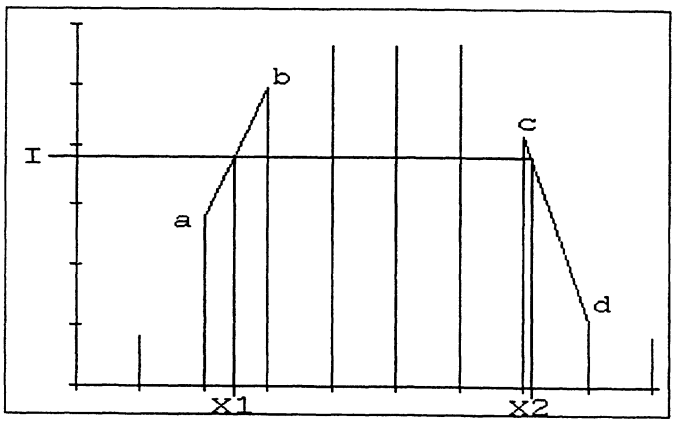

Figure 4. Video Amplitude (Vert. Axis) on Marker Segment, Interpolation (cf. Text)

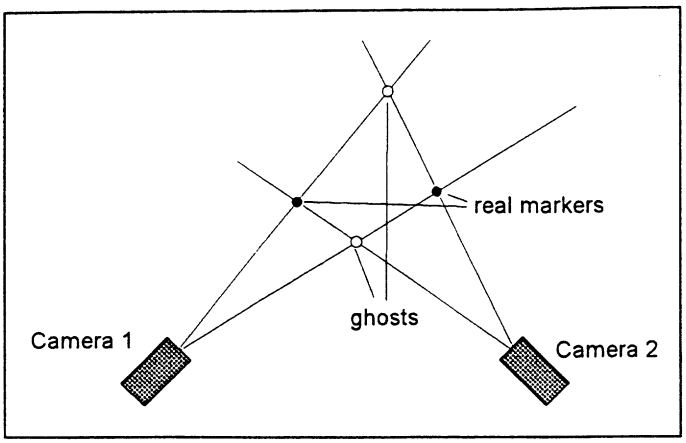

Figure 5. *Ghosts (white) occur in two-camera matching when the cameras (projection centres) and the markers (black) are in the same plane.*

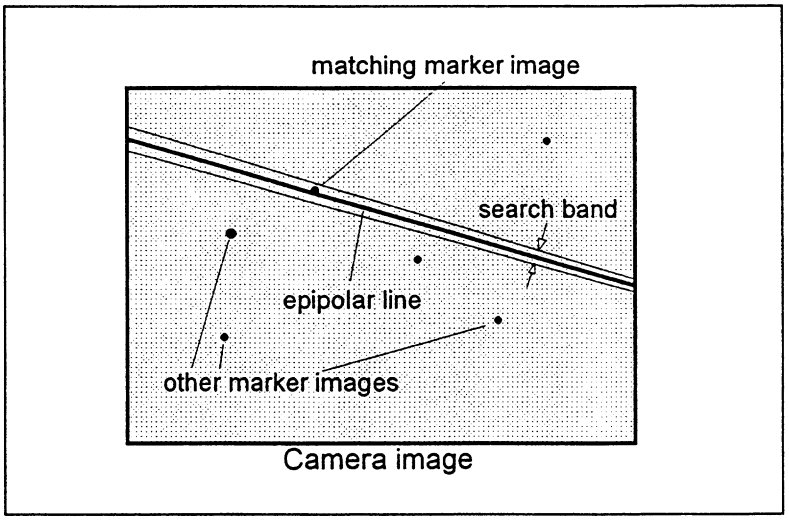

Figure 6. *Matching with epipolar lines.*

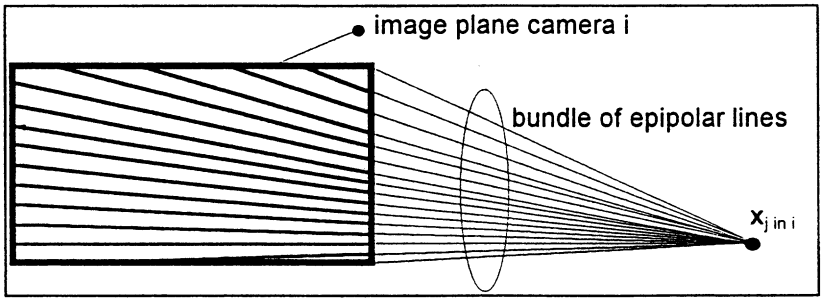

Figure 7. *All epipolar lines pass through the virtual image of the other camera's projection centre,* $\mathbf{x}_{j \text{ in } i}$.

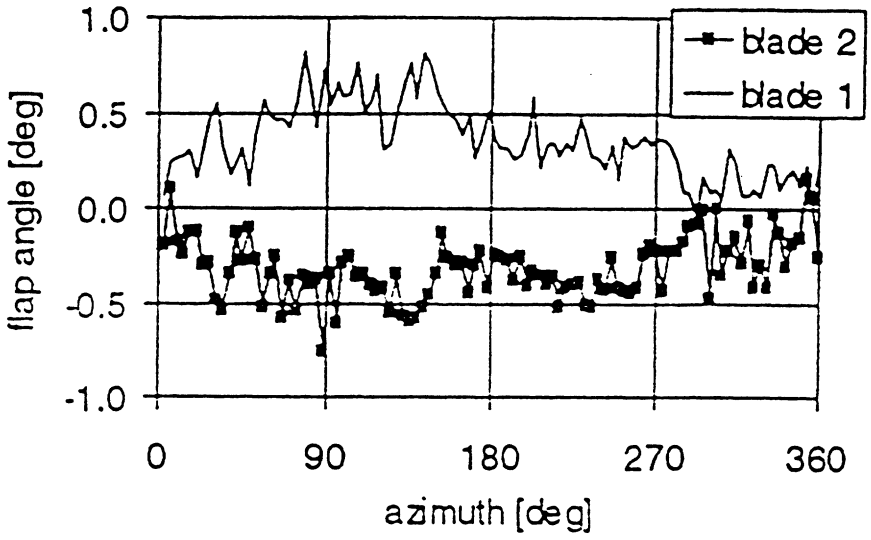

Figure 8: Optically determined flap angles.

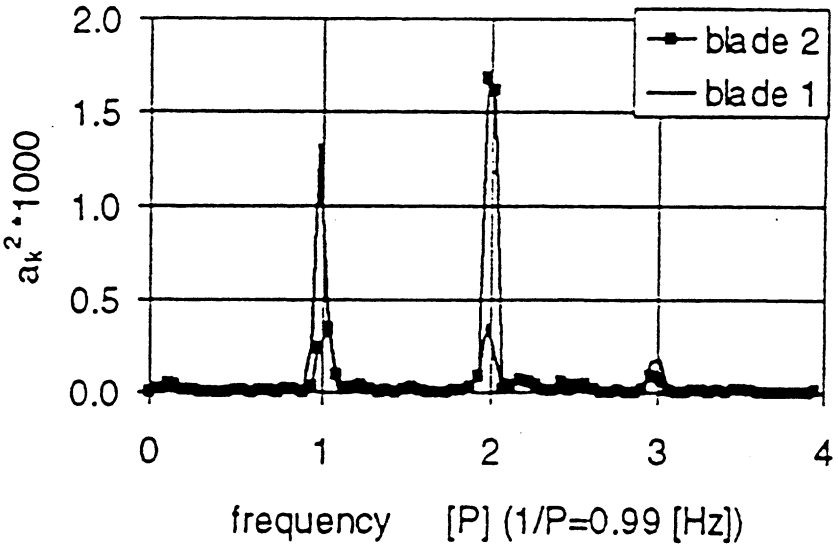

Figure 9: Spectrum of optically determined flap angles determined over 20 rotations..

From: Corten, G.P and J.C. Sabel. Optical motion analysis of wind turbines. The pilot experiment with the Delft 10 [m] diameter wind turbine. In: (Zervos, A., H. Ehmann and P. Helm, eds.) Proc. 1996 European Union Wind Energy Conference and Exhibition. Stephens & Ass. Felmersham UK, ISBN 0952145294, p 875-877, 1996.